Phys Chem Minerals (1986) 13:238–244

PHYSICS AND CHEMISTRY OF MINERALS

Crystal Structure of Magnetite under Pressure

N. Nakagiri[1], M.H. Manghnani[1], L.C. Ming[1], and S. Kimura[2]
[1] Hawaii Institute of Geophysics, University of Hawaii, Honolulu, HI 96822, USA
[2] National Institute for Research in Inorganic Materials, Niiharu-gun, Ibaraki, Japan

Abstract. The crystal structure and the unit-cell parameters of magnetite have been studied at room temperature up to a pressure of 4.5 GPa using a diamond anvil cell and a four-circle X-ray diffractometer. The isothermal bulk modulus (K_T) and its pressure derivative (K'_T) determined by fitting the pressure-volume data to the Murnaghan equation of state are 181(2) GPa and 5.5(15), respectively. The positional parameter u does not vary significantly over the pressure range of this study. The linear compressibilities of the interatomic distances and the bulk moduli of the polyhedra have been calculated from the pressure dependences of the unit-cell edge a and the u parameter. The Bloch equation has been modified to derive a relationship between the Néel temperature and the parameter u. The modified Bloch equation gives a closer agreement with the experimental results than the Weisz equation.

Introduction

Magnetite (Fe_3O_4) has the inverse-spinel structure with space group $Fd3m$ at atmospheric pressure and room temperature. One Fe^{3+} per formula unit is at the tetrahedral site, (1/8, 1/8, 1/8) with equipoint 8(a); the Fe^{2+} and the remaining Fe^{3+} are randomly distributed at the octahedral sites, (1/2, 1/2, 1/2) with equipoint 16(d). The positions (u, u, u) of O atoms are defined by the parameter u with equipoint 32(e). The structure was refined by Hamilton (1958) using neutron diffraction data and by Fleet (1981) using X-ray diffraction data. The value of u was reported as 0.2548(2) and 0.2549(1), respectively.

It is known that magnetite has two other structural modifications: one at low temperature and the other at high pressure. The transition to the low temperature phase occurs at about 120 K. The space group of this phase, *Imma*, proposed by Verwey and co-workers (1941, 1947) was verified by Hamilton (1958). However, recently Iizumi et al. (1982) suggested the space group of this phase to be *Cc* (monoclinic). Samara (1968) studied the pressure dependence of the Verwey transition temperature and found that the transition temperature decreases with pressure.

The structure of the high pressure phase of magnetite observed at 25.0(1) GPa and room temperature was tentatively proposed to be monoclinic (Mao et al. 1974). Recently Huang and Bassett (1985) studied the temperature dependence of this transition to 600 °C, using synchrotron radiation and an energy-dispersive X-ray diffraction technique. They tentatively determined the slope of the phase boundary of the transition as −68 °C/GPa.

Magnetite has a ferrimagnetic ordering of magnetic moments of the iron atoms at atmospheric pressure and room temperature; the Néel temperature T_N is about 850 K. The Fe atoms are too far apart for them to interact directly; they interact through the oxygen atom located between them. The resultant interaction is called a superexchange interaction, and is responsible for the magnetic ordering temperature T_N. The superexchange interaction is, therefore, a function of the interatomic distances and thus depends not only on the lattice parameter a but also on the oxygen positional parameter u.

Samara and Giardini (1969) studied the effect of pressure on the Néel temperature of magnetite to 4.5 GPa, and found that T_N increases linearly with pressure, the slope ($\partial T_N/\partial p$) being 20.5(10) K/GPa. On the basis of Weisz's model (Weisz, 1951), which assumes the spin interaction to be inversely proportional to the interatomic distance, they related the pressure dependence of T_N to the superexchange interaction, and obtained the pressure dependence of the oxygen positional parameter, ($\partial u/\partial p$) as 5.8×10^{-4} GPa^{-1}. However, no experimental data were yet available to evaluate ($\partial u/\partial p$). The present investigation was undertaken to determine ($\partial u/\partial p$) experimentally by refinement of the structure of magnetite under pressure.

Experimental Method

Specimen

The magnetite crystal used in this study was grown along [100] in CO_2 atmosphere at the National Institute for Research in Inorganic Materials, Japan. The growth rate of the crystal was about 4 mm/h. Stoichiometry of the crystal was determined in the following manner. Slices cut from near the two ends (Fig. 1) of the cylindrical crystal were separately crushed, powdered and then heated in air at 1,050 °C for 5 h. The powdered specimens were weighed before and after the heat treatment. The final state was assumed to be

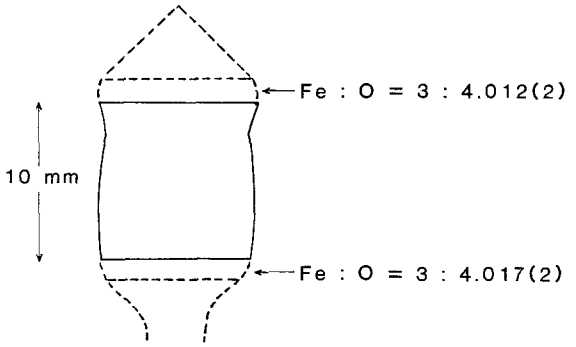

Fig. 1. Shape of the synthetic magnetite single crystal

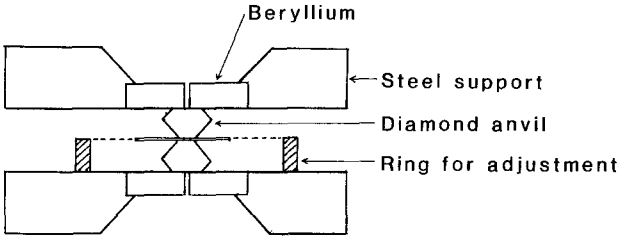

Fig. 2. A cross-section of the diamond anvil cell

Fe:O=1:1.5 and the amount of the reacted oxygen was estimated from the increase in weight. In order to confirm the completion of oxidization, the powdered specimens were heated again at 1,050 °C. No further change in weight was detected. The Fe:O ratios for the two crystal slices were 3:4.017(2) and 3:4.012(2).

Thin plates, 2–3 mm thick, were cut along the (001) plane from the bulk of the crystal, and ground to the desired thickness (60 to 100 μm). The plates were then cut into several small pieces, out of which parallelepiped pieces of the desired dimensions (about $100 \times 100 \times 60$ μm) were selected for high pressure X-ray measurements. A piece of the crystal about $160 \times 130 \times 100$ μm, was selected for X-ray measurements at one bar.

High Pressure Experiments

A Merrill-Bassett type diamond-anvil pressure cell (Merrill and Bassett 1974) was used for high pressure single crystal X-ray diffraction measurements. Pressures up to 4.5 GPa were generated by employing a 0.25 mm-thick stainless steel gasket with 0.3 mm hole to form the sample chamber between the diamond anvil faces. Inside the chamber, the sample was positioned with vacuum grease on the diamond anvil face so that the [001] direction of the crystal was perpendicular to the diamond anvils. A few ruby chips were introduced into the sample chamber to serve as a pressure calibrant. The sample chamber was then filled with a 4:1 methanol:ethanol mixture which is known to maintain a hydrostatic environment up to 10.4 GPa (Piermarini et al. 1973). The pressure on the specimen was measured before and after each X-ray measurement using the ruby fluorescence technique. The average of the two measurements was taken as the pressure on the specimen.

Centering of Crystal on Diffractometer

The pressure cell was mounted on the goniometer head by a suitable attachment. A telescope mounted on the χ frame was positioned to view the crystal in the pressure cell through the holes in the beryllium disks and diamond anvils, and to adjust the position of the crystal along the y and z axes. The x axis was taken parallel to the incident X-ray beam; the z axis in the vertical direction, and y axis perpendicular to x and z when $\omega = \chi = \phi = 0$. Because the telescope was placed along the x axis this arrangement did not permit the adjustment of the crystal along the x axis.

In order to center the crystal on the x axis, a ring was mounted on the pressure cell as shown in Fig. 2. The height of the ring was the same as the center of the crystal on the anvil face. By viewing the upper edge of the ring through the telescope, at $\phi = \pm 90°$, the position of the sample was adjusted on the x axis. The zero position of the ϕ circle was also adjusted so as to coincide the cell axis with the x axis. After centering approximately by means of the ring, the final centering was done by the procedure of King and Finger (1979), which involved measurements of several reflections, each reflection at eight positions in the fixed ϕ mode. In order to obtain reliable data for the deviations in x, y and z axes, each reflection was measured five times, and the average values of 2θ, ω and χ angles were used. After centering the cell on the goniometer, it was taken out for changing and measuring the pressure. After remounting the cell, King and Finger's procedure was used to check whether the crystal was at the center of the goniometer.

X-ray Measurements

The X-ray measurements were made at room temperature. At atmospheric pressure, the bisecting mode was used for determining the unit-cell parameters and for collecting the intensity data. Reflections with 2θ around 40° were used to determine the unit-cell parameters with a sufficiently narrow slit in order to resolve $MoK\alpha_1$ and $MoK\alpha_2$ radiations. The reflections were measured at eight settings in the bisecting mode (Hamilton 1974) to determine the orientation matrix and the unit-cell parameters. The intensity data were collected for reflections up to 60° in 2θ for $h \geqq 0$, $k \geqq 0$ and $l \geqq 0$.

The fixed ϕ mode (King and Finger 1979) was used to determine the unit-cell parameters and to collect the intensity data under pressure. This mode maximizes the available reciprocal space for the Merrill-Bassett diamond anvil cell. Intensity data were collected for all the measurable reflections up to 60° in 2θ.

The $\theta - 2\theta$ scan technique and constant-precision procedure with $\sigma_I/I = 0.01$, where I and σ_I denote the integrated intensity and its standard deviation, respectively, were used to measure the integrated intensities. Two reflections, (400) and (040), were monitored every two hours to check experimental stability; no significant variation was observed during the collection of

intensity data. All the intensities were corrected for absorption by the diamond-anvil cell (Finger and King 1978), and by the crystal using a linear absorption coefficient of 14.65 mm^{-1} for magnetite. Transmission factors for the absorption correction were calculated by Gaussian integration with a $10 \times 10 \times 10$ grid.

Refinement

After making the absorption, Lorentz, and polarization corrections, intensities of the symmetry-related reflections were averaged. The least-squares program RFINE (Finger and Prince 1975) was used for all refinement calculations. Neutral scattering coefficients from Cromer and Mann (1968) and anomalous scattering coefficients from Cromer and Liberman (1970) were used for all the atoms. An isotropic extinction parameter (Zachariasen 1968) was also included in all the refinements.

Results

Pressure Dependence of the Unit Cell Edge and Volume

In the present experiments, a piece of the crystal about $160 \times 130 \times 100$ μm was first selected for X-ray measurements at one bar outside the pressure cell. The unit-cell edge $a = 8.3949(3)$ Å thus obtained agrees well with those reported earlier: 8.3940(5) Å (Abrahams and Calhoun 1953) and 8.3941(7) Å (Fleet 1981). For the pressure runs, four sets of measurements (numbered 1–4 in Table 1) were made on four different chips from the same crystal. Results on the unit-cell edge a, unit-cell volume V at various pressures are listed in Table 1. In the last measurement of the fourth run, the unit-cell edge was determined at one bar with the crystal still inside the pressure cell. The value 8.3978(5) Å obtained is slightly larger than that at one bar measured without the pressure cell. This is most probably caused by systematic errors introduced by the pressure cell. In order to minimize the systematic errors, the value 8.3978(5) Å was used as the unit-cell edge at 1 bar to calculate the volume ratio V/V_0 at various pressures. The V/V_0 values are tabulated in the last column of Table 1 and also plotted in Fig. 3.

Table 1. Pressure dependence of unit-cell edge a, unit-cell volume V, and volume ratio V/V_0 determined in four runs

Run	P, GPa	a, Å	V, Å^3	V/V_0
	0.0001[a]	8.3949 (3)	591.54 (6)	-
1	1.42 (5)	8.3771 (2)	587.87 (4)	0.9926 (2)
	2.00 (5)	8.3686 (2)	586.08 (4)	0.9896 (2)
	2.62 (5)	8.3585 (2)	583.96 (4)	0.9860 (2)
	3.14 (5)	8.3515 (3)	582.50 (6)	0.9836 (2)
	3.67 (5)	8.3453 (1)	581.20 (2)	0.9814 (2)
2	0.74 (5)	8.3856 (1)	589.66 (2)	0.9956 (2)
	1.51 (5)	8.3747 (3)	587.36 (6)	0.9918 (2)
	2.52 (5)	8.3601 (1)	584.30 (2)	0.9866 (2)
3	2.09 (5)	8.3656 (2)	585.45 (4)	0.9885 (2)
	2.76 (5)	8.3557 (2)	583.34 (4)	0.9850 (2)
	3.67 (5)	8.3440 (2)	580.93 (5)	0.9809 (2)
	4.44 (5)	8.3332 (2)	578.68 (5)	0.9771 (2)
	1.55 (5)	8.3740 (2)	587.22 (4)	0.9915 (2)
	0.63 (5)	8.3862 (2)	589.79 (4)	0.9959 (2)
4	0.76 (5)	8.3861 (11)	589.77 (23)	0.9959 (4)
	1.02 (5)	8.3821 (8)	588.92 (17)	0.9944 (3)
	1.14 (5)	8.3805 (5)	588.59 (11)	0.9938 (3)
	1.21 (5)	8.3793 (3)	588.33 (7)	0.9934 (2)
	1.45 (5)	8.3755 (6)	587.53 (13)	0.9921 (3)
	1.71 (5)	8.3725 (5)	586.90 (11)	0.9910 (3)
	1.83 (5)	8.3709 (7)	586.57 (14)	0.9904 (3)
	1.99 (5)	8.3683 (6)	586.02 (12)	0.9895 (3)
	2.03 (5)	8.3675 (2)	585.85 (4)	0.9892 (2)
	2.11 (5)	8.3660 (6)	585.54 (12)	0.9887 (3)
	2.23 (5)	8.3647 (6)	585.26 (13)	0.9882 (3)
	2.31 (5)	8.3640 (6)	585.12 (13)	0.9880 (3)
	2.36 (5)	8.3633 (8)	584.97 (17)	0.9877 (3)
	2.53 (5)	8.3607 (11)	584.42 (23)	0.9868 (4)
	2.84 (5)	8.3555 (2)	583.33 (4)	0.9850 (2)
	3.08 (5)	8.3530 (6)	582.80 (13)	0.9841 (3)
	3.31 (5)	8.3496 (5)	582.10 (10)	0.9829 (3)
	4.06 (5)	8.3383 (3)	579.73 (6)	0.9789 (2)
	0.72 (5)	8.3879 (3)	590.15 (6)	0.9965 (2)
	0.65 (5)	8.3877 (3)	590.10 (6)	0.9964 (2)
	0.02 (5)	8.3976 (6)	592.11 (13)	0.9998 (3)
	0.0001[b]	8.3978 (5)	592.24 (12)	-

The data are presented in the same sequence as that of measurements. Parenthesized figures represent standard deviations of the least units cited

[a] Measured without the pressure cell

[b] Measured in the pressure cell after the pressure was completely released. This value is used to calculate the volume ratio shown in the last column

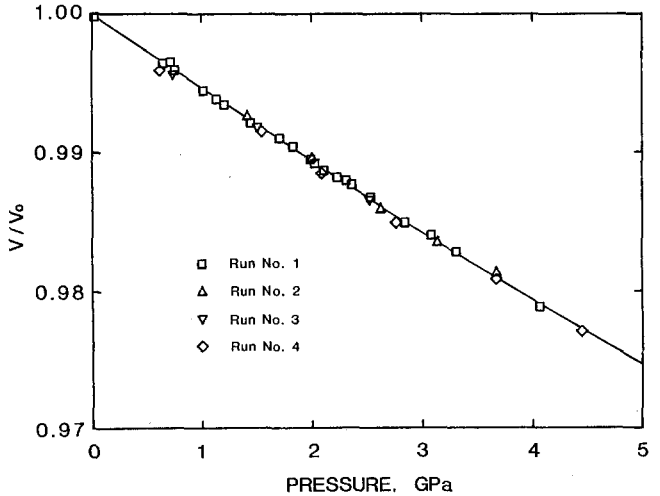

Fig. 3. The pressure-volume data for magnetite. The solid line is the regression curve obtained by fitting the data to the Murnaghan equation

The pressure-volume data fitted to the Murnaghan equation give the values of K_T and K'_T as 181(2) GPa and 5.5(15), respectively. The present value of K_T lies in the range 139 to 185 GPa reported by various investigators (see Table 1 of Wilburn and Bassett 1977).

Bridgman (1949) reported a cusp in the compression curve at 2.21 GPa, at which the bulk modulus decreased by about 4.7 percent. However, such a cusp was not observed in the present experiments and the compression curve is smooth up to 4.5 GPa.

Table 2. Refined parameters

Pressure (GPa)	0.0001	0.0001[a]	0.63 (5)	1.55 (5)	2.09 (5)	2.76 (5)	3.67 (3)	4.44 (5)
Number of reflections	123	147	34	32	31	32	31	33
R (%)[b]	2.6	3.3	2.6	2.8	3.3	2.6	3.1	3.4
wR (%)[c]	2.4	2.4	2.1	2.4	3.0	2.2	2.7	2.6
Extinct ($\times 10^{-5}$)	2.4 (1)	13.2 (10)	1.0 (2)	1.0 (3)	1.1 (4)	0.9 (2)	1.0 (3)	0.9 (3)
Oxygen u	0.2548 (2)	0.2549 (1)	0.2539 (5)	0.2540 (6)	0.2537 (8)	0.2547 (6)	0.2535 (7)	0.2540 (7)
B_{Fe}(tet)[d]	0.53 (2)	0.34 (2)	0.90 (7)	0.85 (9)	0.91 (11)	0.77 (8)	0.85 (10)	0.86 (9)
B_{Fe}(oct)	0.82 (3)	0.46 (2)	1.09 (15)	1.04 (20)	1.17 (26)	0.83 (19)	1.27 (23)	1.04 (23)
B_0	0.56 (8)	0.49 (3)	0.54 (45)	0.76 (59)	0.27 (73)	1.22 (52)	0.27 (62)	0.89 (66)

Parenthesized figures represent standard deviations of least unit cited

[a] Fleet (1981)

[b] $R=\sum||F_{obs}|-|F_{calc}||/\sum|F_{obs}|$

[c] $wR=[\sum w(F_{obs}-F_{calc})^2/\sum wF_{obs}^2]^{1/2}$

[d] Isotropic temperature factor equivalent to the anisotropic values

Pressure Dependence of the Oxygen Positional Parameter

The refinement conditions and the refined parameters are listed in Table 2. Also shown for comparison are Fleet's (1981) data at one bar. After averaging symmetrically equivalent reflections, the number of independent reflections observed is 123 at one bar and 31 to 34 at high pressures. The R values range from 2.6 to 3.4, and the weighted R values range from 2.1 to 3.0. The oxygen positional parameter, u, 0.2548(2) at 1 bar is in good agreement with the values 0.2549(1) and 0.2548(2) reported by Fleet (1981) and by Hamilton (1958), respectively. The values of u obtained at different pressures have been plotted in Figure 4(a). The pressure dependence of u was determined by fitting the u-p data to an equation of the type

$$u=u_0+(\partial u/\partial p)p.$$

As the systematic errors may have been introduced by the pressure cell and by the limited number of reflections at high pressures in the determination of u, the one-bar value of u determined outside the pressure cell was not included in the analysis of the data. The following results were obtained:

$$u_0=0.2540(4) \quad \text{and} \quad (\partial u/\partial p)=-1(15)\times 10^{-5}\ \text{GPa}^{-1},$$

the latter indicating that u does not vary significantly with pressure.

The temperature factor B for Fe at the tetrahedral site, 0.53(2), and that for oxygen, 0.56(8), also compare well with Fleet's values 0.34(2) and 0.49(3). However, the temperature factor for Fe at the octahedral site, 0.82(3), is larger than Fleet's value 0.46(2). As shown in Table 2, the values of the temperature factor at high pressures do not show any systematic trend.

Pressure Dependence of the Interatomic Distances and Angle

The interatomic distances in the spinel structure expressed in terms of the unit-cell edge a and the oxygen positional parameter u are presented in Table 3. The interatomic distances were calculated using the values $a=8.3949(3)$ Å and $u=0.2548(2)$, obtained in the present

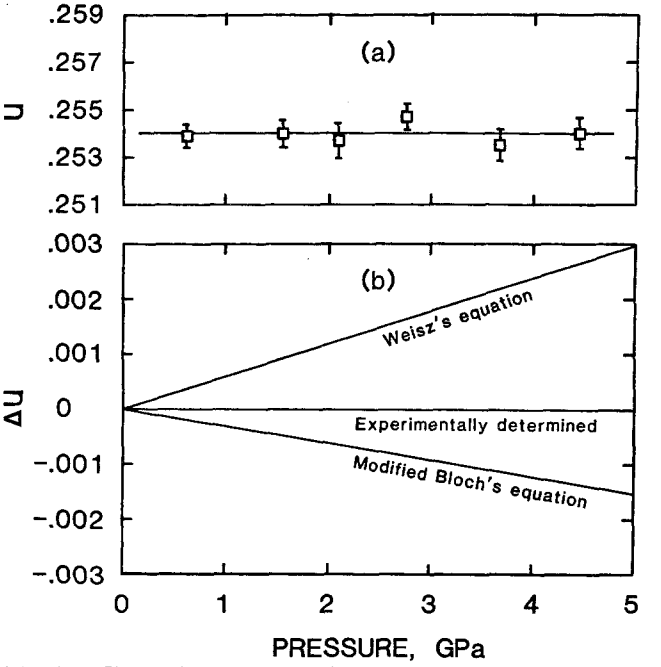

Fig. 4. **a** The variation of u with pressure; **b** A comparison of the calculated and the experimental values of Δu as a function of pressure

experiments at atmospheric pressure. The compression of each interatomic distance can be derived from the expression given in Table 3. The distances $A-A$, $A-B$ and $B-B$, where A and B represent Fe atoms in the tetrahedral and octahedral sites, respectively, are independent of u, so that the compressibilities of these distances are the same as the linear compressibility β_a of the unit-cell edge, i.e., $1.84(2)\times 10^{-3}\,\text{GPa}^{-1}$. The other interatomic distances $A-X$, $B-X$ and $X-X$, where X represents the oxygen atom, depend on both a and u. The linear compressibilities can be expressed as follows:

$$\beta(r_{AX})=-\frac{1}{r_{AX}}\left(\frac{\partial r_{AX}}{\partial p}\right)$$
$$=-\frac{1}{a}\left(\frac{\partial a}{\partial p}\right)-\frac{1}{u-0.125}\left(\frac{\partial u}{\partial p}\right) \quad (1)$$

Table 3. Linear compressibilities of interatomic distances of magnetite. A, B and X represent tetrahedral site Fe, octahedral site Fe and O, respectively

Atomic pair	Interatomic distance	Interatomic distance (ambient pressure)	Compressibility, 10^{-3}/GPa	Comments
AA	$a\sqrt{3}/4 \equiv r_{AA}$	3.6351 (1)	1.84 (2)	tet-tet cation separation
AB	$a\sqrt{11}/8 \equiv r_{AB}$	3.4803 (1)	1.84 (2)	tet-oct cation separation
BB	$a\sqrt{2}/4 \equiv r_{BB}$	2.9680 (1)	1.84 (2)	oct-oct cation separation
AX	$a\sqrt{3}(u-0.125) \equiv r_{AX}$	1.8873 (29)	1.9 (12)	tet bond
BX	$a(3u^2-2u+0.375)^{1/2} \equiv r_{BX}$	2.0592 (16)	1.8 (6)	oct bond
XX	$a\sqrt{2}(2u-0.25) \equiv r_{Xt}$	3.0820 (48)	1.9 (12)	tet edge
XX	$a\sqrt{2}(0.75-2u) \equiv r_{Xs}$	2.8541 (47)	1.8 (13)	shared oct edge
XX	$a(4u^2-2u+0.375)^{1/2} \equiv r_{Xu}$	2.9691 (1)	1.84 (3)	unshared oct edge

$$\beta(r_{BX}) = -\frac{1}{r_{BX}}\left(\frac{\partial r_{BX}}{\partial p}\right) = -\frac{1}{a}\left(\frac{\partial a}{\partial p}\right) - \frac{3u-1}{3u^2-2u+0.375}\left(\frac{\partial u}{\partial p}\right) \quad (2)$$

$$\beta(r_{Xt}) = -\frac{1}{r_{Xt}}\left(\frac{\partial r_{Xt}}{\partial p}\right) = -\frac{1}{a}\left(\frac{\partial a}{\partial p}\right) - \frac{1}{u-0.125}\left(\frac{\partial u}{\partial p}\right) \quad (3)$$

$$\beta(r_{Xs}) = -\frac{1}{r_{Xs}}\left(\frac{\partial r_{Xs}}{\partial p}\right) = -\frac{1}{a}\left(\frac{\partial a}{\partial p}\right) + \frac{1}{0.375-u}\left(\frac{\partial u}{\partial p}\right) \quad (4)$$

$$\beta(r_{Xu}) = -\frac{1}{r_{Xu}}\left(\frac{\partial r_{Xu}}{\partial p}\right) = -\frac{1}{a}\left(\frac{\partial a}{\partial p}\right) - \frac{4u-1}{4u^2-2u+0.375}\left(\frac{\partial u}{\partial p}\right). \quad (5)$$

The first term on the right hand side in the above equations, $-(1/a)(\partial a/\partial p)$, is simply the compressibility of the unit-cell edge a, i.e., β_a. Substituting the values of β_a, $(\partial u/\partial p)$, a and u in these equations, the compressibilities of the interatomic distances were obtained. Because of the small pressure-dependence of u, the linear compressibilities of the interatomic distances have similar values. Since r_{AX}, r_{Xt} and r_{Xs} depend significantly on u, the large standard deviation in $(\partial u/\partial p)$ causes the large uncertainties in their linear compressibilities. In order to determine the linear compressibilities more precisely, we should collect data at higher pressures or achieve a better precision in the data.

The bond angle $A-X-B$, (i.e., α), which is associated with the superexchange interaction, can be calculated from u as follows:

$$\cos\alpha = \frac{3u-1}{\sqrt{3}(3u^2-2u+0.375)^{\frac{1}{2}}}. \quad (6)$$

The value of α is 123.68(7) at atmospheric pressure. The pressure dependence of this angle was calculated to be $6(88)\times10^{-5}$ deg/GPa. The change in the angle is thus negligibly small.

Polyhedron Bulk Modulus

The volume V_{tet} of the tetrahedra and V_{oct} of the octahedra can be expressed in terms of the tetrahedral edge r_{Xt}, the shared octahedral edge r_{Xs}, and the unshared octahedral edge r_{Xu} as follows:

$$V_{tet} = (\sqrt{2}/12) r_{Xt}^3 \quad (7)$$

and

$$V_{oct} = (1/3) r_{Xu}^2 (3r_{Xs}^2 - r_{Xu}^2)^{1/2}. \quad (8)$$

Using the values of r_{Xt}, r_{Xs} and r_{Xu} (Table 3), the following values were obtained for the volumes at atmospheric pressure: $V_{tet} = 3.45(2)$ Å^3 and $V_{oct} = 11.61(3)$ Å^3. The compressibilities and bulk moduli can be derived by differentiating Eqs. (7) and (8). The results thus obtained are

$$\beta_{tet} = 5.8(35)\times10^{-3}\,\text{GPa}^{-1}; \qquad K_{tet} = 1.7(10)\times10^2\,\text{GPa}$$

and

$$\beta_{oct} = 5.4(20)\times10^{-3}\,\text{GPa}^{-1}; \qquad K_{oct} = 2.0(8)\times10^2\,\text{GPa}.$$

Discussion

Pressure Dependence of u

There are two equations relating the volume (or interatomic distance) to Néel temperature T_N in superexchange magnetism. The first of these is an empirical relation suggested by Bloch (1966), known as the 10/3 law, and is given by

$$(\partial \ln T_N/\partial p) = (10/3)\beta_V \quad (9)$$

where p and β_V denote the pressure and isothermal volume compressibility. The other equation relating T_N to interatomic distance d in spinel (Weisz 1951) is:

$$k T_N = C_1 S_A S_B e^{-C_2 d} \quad (10)$$

where k is Boltzmann's constant, S_A and S_B are the electric spins of A and B atoms, respectively; d is the distance $A-X-B$ which is equal to $r_{AX}+r_{BX}$ in the present notation; C_1 and C_2 determined empirically (Weisz 1951) are 5.04×10^{-3} erg and 7 Å^{-1}, respectively. This equation was derived on the assumption that the spin interaction in the inverse spinels is inversely

proportional to the distance between A and B atoms to explain the dependence of the exchange interaction on the interatomic distance.

The interaction between A and B is prominent in magnetite and the interactions between A and A, and between B and B are negligible (Samara and Giardini 1969). Also, the magnetic moments of A and B atoms are independent of pressure (Samara 1969). Further, the present results clearly indicate that the change in the bond angle $A-X-B$ is negligibly small. Consequently, the interaction is dependent only on the distances r_{AX} and r_{BX}.

Samara and Giardini (1969) estimated the value of $(\partial u/\partial p)$, from Weisz's equation (10) in the following manner. Differentiating Eq. (10), and equating d to $r_{AX}+r_{BX}=(0.3765+0.732u)a$, (a different definition of u was used by Samara and Giardini); they obtained:

$$(\partial \ln T_N/\partial p) = -C_2(\partial d/\partial p) \tag{11}$$

$$\left(\frac{\partial u}{\partial p}\right) = -\frac{1}{0.732a}\left\{\frac{1}{C_2}\left(\frac{\partial \ln T_N}{\partial p}\right) - (0.192+0.732u)\left(\frac{\partial a}{\partial p}\right)\right\}. \tag{12}$$

Substituting

$(\partial \ln T_N/\partial p) = 2.42\times10^{-2}\,\mathrm{GPa}^{-1}$ (Samara and Giardini 1969),

$(\partial a/\partial p) = -1.5\times10^{-2}$ Å/GPa (Mao 1967),

$u=0.254$ and $a=8.390$ Å,

Samara and Giardini (1969) obtained $(\partial u/\partial p)=5.8\times10^{-4}\,\mathrm{GPa}^{-1}$. This value is compared with the observed value in Fig. 4b. The Weisz equation does not appear to predict well the pressure dependence of u.

We have attempted to use Bloch's equation in order to calculate the pressure dependence of u. It should be pointed out that Bloch's equation is empirical, though it has some theoretical implications. That is, if we assume that the interactions between A and X, and between B and X are both proportional to W ($2W$ is the band width), the superexchange interaction between A and B is proportional to W^2. Then, using Heine's (1967) relation

$$(\partial \ln W/\partial \ln V) = -5/3 \tag{13}$$

Bloch's equation (9) can be rewritten as follows:

$$(\partial \ln T_N/\partial p) = 2\beta_V(-\partial \ln W/\partial \ln V) = (10/3)\beta_V.$$

This equation gives a relation between T_N and volume. It is apparent that we cannot use this equation for the spinel structure, because the superexchange interaction depends on associated interatomic distances, which in turn are dependent on both the volume (that is, the unit-cell edge) and the oxygen positional parameter. We, therefore, modify the Eq. (9), such that it contains r_{AX} and r_{BX} as follows. The volume compressibility is three times the linear compressibility of the unit-cell edge a, β_a. Therefore, the Eq. (9) becomes

$$(\partial \ln T_N/\partial p) = 10\beta_a \quad (\because \beta_V = 3\beta_a). \tag{14}$$

Then, the linear compressibility β_a is replaced by $\{\beta(r_{AX})+\beta(r_{BX})\}/2$, where $\beta(r_{AX})$ and $\beta(r_{BX})$ denote the compressibilities of the distances r_{AX} and r_{BX}, respectively. This replacement leads to the relation

$$(\partial \ln T_N/\partial p) = 5\{\beta(r_{AX})+\beta(r_{BX})\}, \tag{15}$$

which indicates that the superexchange interaction depends on the distances between A and X, and between B and X, independently. Thus the relation between the pressure derivative of T_N and u is obtained as follows:

$$\left(\frac{\partial \ln T_N}{\partial p}\right) = 10\beta_a - 5\left(\frac{1}{u-0.125}+\frac{3u-1}{3u^2-2u+0.375)}\right)\left(\frac{\partial u}{\partial p}\right). \tag{16}$$

Substituting the following values in (16):

$(\partial \ln T_N/\partial p) = 2.42\times10^{-2}\,\mathrm{GPa}^{-1}$,

$\beta_a = 1.84\times10^{-3}\,\mathrm{GPa}^{-1}$,

and

$u=0.2548$,

where the value of $(\partial \ln T_N/\partial p)$ is from Samara and Giardini (1969) and the other values are from the present experimental results, we obtain

$$(\partial u/\partial p) = -3.1\times10^{-4}\,\mathrm{GPa}^{-1}. \tag{17}$$

This calculated negative value for $(\partial u/\partial p)$ is in contrast to the positive value $5.8\times10^{-4}\,\mathrm{GPa}^{-1}$ calculated by Samara and Giardini. To compare the calculated values with the present experimental results, three lines representing the gradients are drawn in the Δu–p plane (Fig. 4b). The modified Bloch equation appears to agree with the experimental results more closely than the Weisz equation.

Furthermore, it is to be noted that the Weisz equation contains two parameters C_1 and C_2 which are determined empirically, while the Bloch equation does not contain any such parameters. These factors together with the present experimental results seem to favor the Bloch equation in formulating the relationship between $(\partial T_N/\partial p)$ and $(\partial u/\partial p)$. More experimental data on both $(\partial T_N/\partial p)$ and $(\partial u/\partial p)$ for some other isostructural ferrimagnetic materials are, therefore, needed for evaluating the validity of the Bloch equation.

Conclusions

1. The isothermal bulk modulus K_T and its pressure derivative K'_T of a synthetic magnetite crystal have been determined to be 181 (2) GPa and 5.5 (15), respectively, by fitting the present pressure-volume data to the Murnaghan equation of state.

2. The crystal structure of magnetite has been refined at various high pressures. The variation of the positional parameter with pressure has been determined as $-1\,(15)\times10^{-5}\,\mathrm{GPa}^{-1}$.

3. The Bloch equation has been modified to calculate the pressure dependence of the oxygen positional parameter. The calculated value has a negative sign while that reported by Samara and Giardini using the Weisz equation has a positive sign. The present calculations seem to agree with the experimental results better than those of Samara and Giardini.

Acknowledgement. This research was supported by NSF grant EAR81-16280 and EAR82-19201, Hawaii Natural Energy Institute, and the University of Hawaii. John Balogh designed and fabricated most of the components used in the X-ray diffraction work. We thank Larry W. Finger and Barry R. Lienert for help in computer interfacing and programming, and Diane Henderson for editorial comments on the manuscript. We also thank Robert M. Hazen and the referee of the paper for their constructive comments and helpful suggestions. This is Hawaii Institute of Geophysics Contribution no. 1759.

References

Abrahams SC, Calhoun BC (1953) The low-temperature transition in magnetite. Acta Crystallogr 6:105–106

Bloch D (1966) The 10/3 law for the volume dependence of superexchange. J Phys Chem Solids 27:881–885

Bridgman PW (1949) Linear compression to 30,000 kg/cm^2 including relatively incompressible substances. Proc Am Acad Arts Sci 77:187–234

Cromer DT, Liberman D (1970) Relativistic calculation of anomalous scattering factors for X rays. J Chem Phys 53:1892–1893

Cromer DT, Mann JB (1968) X-ray scattering factors computed from numerical Hartree-Fock wave functions. Acta Crystallogr A24:321–324

Finger LW, Prince E (1975) A system of Fortran IV, computer programs for crystal structure computations. Nat. Bur. Stand. (U.S.) Tec. Note 854

Finger LW, King H (1978) A revised method of operation of the single-crystal diamond cell and refinement of the structure of NaCl at 32 kbar. Am Mineral 63:337–342

Fleet ME (1981) The structure of magnetite. Acta Crystallogr B37:917–920

Hamilton WC (1958) Neutron diffraction investigation of the 119 °K transition in magnetite. Phys Rev 110:1050–1057

Hamilton WC (1974) Angle settings for four-circle diffractometers. In: International Tables for X-ray Crystallography Vol IV. International Union of Crystallographers, Birmingham, England, 273–284

Heine V (1967) *S–d* interaction in transition metals. Phys Rev 153:673–682

Huang E, Bassett WA (1985) Rapid determination of Fe_3O_4 phase diagram by synchrotron radiation. In press

Iizumi, M., Koetzle TF, Shirane G, Chikazumi S, Matsui M, Todo S (1982) Structure of magnetite (Fe_3O_4) below the Verwey transition temperature. Acta Crystallogr B38:2121–2133

King HE, Finger LW (1979) Diffracted beam crystal centering and its application to high-pressure crystallography. J Appl Crystallogr 12:374–378

Mao HK (1967) Ph.D. thesis, University of Rochester, (unpublished)

Mao HK, Takahashi T, Bassett WA, Kinsland GL, Merrill L (1974) Isothermal compression of magnetite to 320 kbar and pressure-induced phase transition. J Geophys Res 79:1061–1069

Merrill L, Bassett WA (1974) Miniature diamond anvil pressure cell for single crystal diffraction studies. Rev Sci Instrum 45:290–294

Piermarini GJ, Block S, Barnett JD (1973) Hydrostatic limits in liquids and solids to 100 kbar. J Appl Phys 44:5337–5382

Samara GA (1968) Effect of pressure on the metal-nonmetal transition and conductivity of Fe_3O_4. Phys Rev Lett 21:795–797

Samara GA (1969) Effects of pressure on the magnetic properties of magnetite. Bull Am Phys Soc 14:308

Samara GA, Giardini AA (1969) Effect of pressure on the Neel temperature of magnetite. Phys Rev 186:577–580

Verwey EJ, Haayman PW (1941) Electronic conductivity and transition point of magnetite (Fe_3O_4). Physica 8:979–987

Verwey EJ, Haayman PW, Romeijn FC (1947) Physical properties and cation arrangement of oxides with spinel structures, II Electron conductivity. J Chem Phys 15:181–187

Weisz RS (1951) Interatomic distances and ferromagnetism in spinels. Phys Rev 84:379

Wilburn DR, Bassett WA (1977) Isothermal compression of magnetite (Fe_3O_4) up to 70 kbar under hydrostatic conditions. High Temp-High Pressures 9:35–39

Zachariasen WH (1968) Extinction and Borrmann effect in mosaic crystals. Acta Crystallogr A24:421–424

Received August 7, 1985